Synthesis and photocatalytic activity for TiO_2 nanoparticles as air purification

Adawiya Haider [1], *Riyad* Al- Anbari[1], *Ghadah* Kadhim[1] , *Zainab* Jameel[1]

[1]University of Technology, Baghdad, Iraq

Abstract. In the present work, titanium dioxide (TiO2) nanoparticles (NP's) were prepared using sol-gel process from Titanium Tetrachloride (TiCl4) as a precursor with calcinations at two temperatures (500 and 900) °C. The effect of calcinations temperatures on the structural, optical, morphological and Root Mean Square (roughness) properties were investigated by means of Scanning Electron Microscopy, X-ray Diffraction (XRD), and Atomic Force Microscopy (AFM). Bacterial inactivation was evaluated using TiO2-coated Petri dishes. A thin layer of photocatalytic TiO2 powder was deposited on glass substrate in order to investigate the self-cleaning effect of TiO2 nanoparticles in indoor and outdoor applications. Ultra-hydrophilicity was assessed by measuring the contact angle and it evaluated photolysis properties through the degradation of potassium permanganate (KMnO4) under direct sunlight. XRD analysis indicated that the structure of TiO2 was anatase at 500 °C and rutile at 900 °C calcination temperatures. As the calcination temperature increases, the crystallinity is improved and the crystallite size becomes larger. Coated films of TiO2 made the has permeability, low water contact angle and good optical activity. These are properties essential for the application of the surface of the self-cleaning. The final results illustrate that titanium dioxide can be used in the build materials to produce coated surfaces in order to minimize air pollutants that are placed in microbiologically sensitive circumference like hospitals and the food factory.

1 Introduction

Ecological pollution, such as dirty water or contaminated air, has become a universal problem that affects human health. Typical polluting sources are toxic organic molecules or exhausted gas compounds that are released from household waste, livestock waste and local industries [1, 2, 3, 4, 5]. Growth and deposition of microbes on surfaces such as walls, windows and tables also pose a substantial threat to human health. Continual exposure to these pollutants can lead to varied health troubles like irritations and toxic effects, and other various respiratory or skin diseases. Most studies on photocatalysts show that it is a better technique for biodegradable organic pollutants using clean solar energy without generating any harmful products [6]. Photocatalytic technique is an effective purification process capable of disrupting a wide range of harmful microorganisms in various media. It is safe, non-toxic, and relatively inexpensive method of disinfection which allows the ability to adapt to use in many applications such as air purification, water purification, and treatment of hazardous waste, water purification [7, 8, 9]. This technique can be envisaged as one of the most promising Advanced Oxidation Process (AOPs) due to its specific advantages, such as bland reaction conditions, the possibility of using molecular oxygen as oxidant species, the total mineralization of pollutants into substances innocuous to the environment. Photocatalysis is based on the interaction between semiconductor materials and light by considering that 'free' light from the sun, electron will be excited from the valance band to the conduction band thus creating an electron-hole pair, the holes (h+) and hydroxyl radicals (OH•) generated in the valence band, also electrons and superoxide anions (O2 •-) generated in the conduction band, irradiated TiO2 photocatalysts can decompose and mineralize organic compounds by a series of oxidation reactions leading to carbon dioxide [10, 11]. The idea of using solar light energy as resource to clean up the environment is an ideal and promising approach.

*Corresponding Author: 100081@uotechnology.edu.iq

Among various oxide photocatalysts, the preparation, characterization and applications of semiconductor titanium dioxide (TiO2) have become a research hot spot. The photocatalytic oxidation (PCO) using titanium dioxide is an efficient technology for the degradation of many pollutants [12, 13, 14, 15]. It has also been known that the TiO2 shows the hydrophilicity due to the photocatalytic nature, the water tends to sheet across this surface rather than forming droplets [16]. This makes the surface anti-fogging and easily washable. TiO2 photocatalyst has good chemical stability, relative low price, wide availability, non-toxicity and it has strong oxidizing power [17, 18, 19, 20, 21, 22].

Super-hydrophilicity is a phenomenon that occurs when TiO2 coated surface is illuminated by UV radiation. The hydrophilic surface has a very small contact angle ($\theta \leq 5o$) that allows water to sheet across this surface rather than forming droplets. This makes the surface anti-fogging and easily washable [23].

In this work, the synthetic method of nanostructure, a Titanium dioxide (TiO2) based on TiCl4, has been synthesized by sol-gel method and thermally treated at two temperatures. The effect of thermal treatment on the structural and morphological properties of the material was investigated by means of SEM, XRD and AFM and measuring the contact angle of water drop on the films by spin coating technique to evaluate the hydrophilicity property.

2 Experimental section

2.1 Synthesis of TiO_2 nanoparticles

TiO_2 Nanaparticles was prepared by Sol-Gel method using Titanium Tetrachloride ($TiCl_4$) as precursor of TiO_2 as described in (Adawyia et al. 2017).

2.2 *Characterization*

The prepared nanoparticles were characterized for the crystalline phase by X-ray diffraction using (XRD-6000 2kw type), at room temperature, operating at 40 kV and 30 mA, Cu (1.54060 A). The morphological changes of prepared TiO_2 nanoparticles at different calcination temperatures were analyzed using Scanning Electron Microscopy (SEM, Tescan VEGA3 SB). Zeta potential (ZetaPlus) was used to measure Zeta potential of the particles in liquid suspension using Electrophoretic Light Scattering (ELS) technique with the range between -250 mV to 250 mV (sample dependent). The size of the prepared TiO_2 nanoparticles was measured by using (Particle size analyzer, 90Plus). Fourier Transform Infrared spectroscopy (FTIR) has been extensively used for identifying the various functional groups.

3 Results and discussion

3.1 X-ray diffraction (XRD)

Precise metal composition and grain size of TiO_2NP's were determined by XRD.

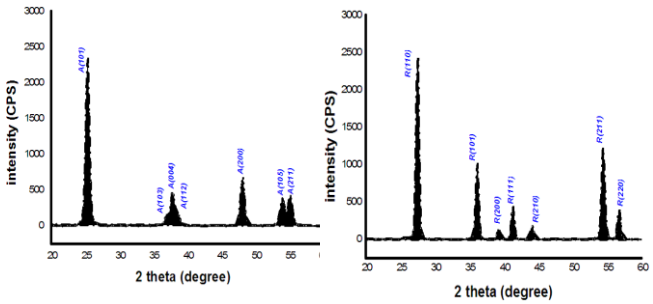

Fig- 1 presents the XRD pattern of TiO2 nanoparticles obtained by sol gel method and calcined at different temperatures.

Crystallite size was obtained by Scherrer's formula given by equation:

$D=K\lambda/(\beta\cos\theta)$ (1)

Where K is a constant that depends on the crystallite shape (0.9, with the assumption of spherical particles) [24], λ is the X-ray wavelength, β is the full width at half maximum of the selected peak and θ is the Bragg's angle of diffraction for the peak.

The XRD patterns results indicate that the structure of TiO_2 was anatase at calcination temperatures at 500 ^oC, rutile at 900 ^oC. The anatase phase was identified at 2θ values of 25.4^o, 38.1^o, 48.2^o, 53.9^o and 55.1^o, corresponds to the crystal planes of (101), (004), (200), and (105) respectively, which are in agreement with the standard XRD pattern (JCPDS files No. 21-1272). Rutile phase was also identified at 2θ values of 27.5^o, 36.1^o, 41.3^o, 44.2^o and 55.5^o corresponding to the crystal planes of (110), (101), (200), (111), (210), (211), and (220) respectively,in agreement with the standard XRD pattern (JCPDS files No. 21-1276).

Table 1.Effect of calcination temperatures on the crystallite sizes and phase content of TiO2 nanoparticles

Calcination temperature (^oC)	Phase [a]	2θ (Deg.)	β(FWHM) (Deg.)	Grain sized [b] (nm)	WR %
500	A	25.4005	0.6209	12.5	0
		48.1266	0.6902	12.45	
		37.9087	0.8796	11	
900	R	27.5443	0.5243	16.9	100
		54.5425	0.5611	16.7	
		36.2899	0.4991	18	

[a] A stands for anatase and R stands for rutile. [b] The crystallite size was calculated by using Sherrer's equation.

3.2 Scanning Electron Microscopy (SEM)

The micrographs SEM images of TiO2 nanoparticles were prepared at different calcination temperatures as shown in Figure 2. (Figure 2a) shows TiO2 nanoparticles calcined at 500°C have roughly spherical spongy shape with small size nanoparticles around the range of less than 10 nm. When the temperature increases, the sizes become bigger and the agglomeration becomes significant. Further increase in temperature up to 900°C, TiO_2 nanoparticles exhibited non-uniform particles shape due to the agglomeration of initial particles with increase in crystalline size. These results are in agreement with XRD results that showed that the particles size of the anatase phase is smaller than rutile phase due to aggregation of nanoparticles with increased calcination temperature.

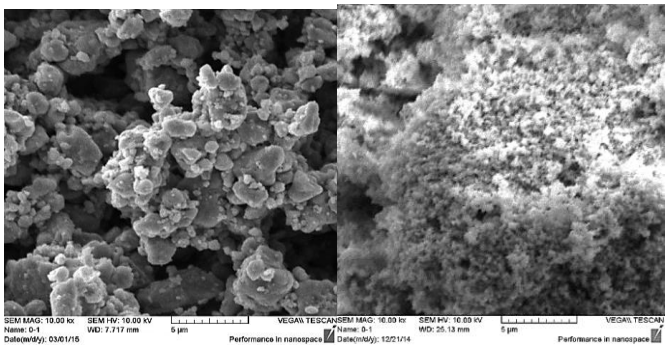

Fig-2 SEM images of TiO2 nanoparticles calcined at (a): 500°C, (b) 900°C

3.3 Zeta potential surface charge for TiO2 nanoparticles

Zeta potential surface charge for TiO2 nanoparticles is illustrated in Figure (3). According to ASTM Standard (D 4187–82), illustrated in Table (3), TiO2 collides prepared at 500°C have good stability. An excellent stability has been found with TiO2 collides prepared at 900°C.

Table 2. List of Zeta potential, Frequency, Frequency shift, and Mobility data for TiO2 nanoparticles calcined at different calcination temperatures

Tio2 Samples Calcined At	Zeta Potential (Mv)	Frequency (Hz)	Frequency Shift (Hz)	Mobility (μ/S)/(V/Cm)
500 °C	-52.95	151.29	-98.71	-12.80
900 °C	-76.12	147.96	-102.04	-13.47

Table 3. ASTM Standard (D 4187–82)

Zeta potential mV	Stability behavior of the colloid
from 0 to ±5,	Rapid coagulation or flocculation
from ±10 to ±30	Incipient instability
from ±30 to ±40	Moderate stability
from ±40 to ±60	Good stability
more than ±61	Excellent stability

3.4 Particle Size Analyzer

Particle size analysis illustrated in Table 4 shows that when the calcination temperature was increased the crystallites tend to agglomerate leading to the formation of bigger particles. This result is in agreement with XRD and SEM results.

3.5 Atomic force microscopy (AFM)

The surface morphology was studied by means of AFM (Atomic force microscopy). Figure 3 shows two- and three-dimensional AFM images of the TiO_2 coatings calcined at 500 and 900 °C, respectively. It was observed that, at different calcination treatment temperatures, the surface morphologies and roughness of the TiO_2 surface are obviously different. As it can be seen from Figure 3a (coating treated at 500 °C), a granular microstructure and a flat texture, with the lowest surface roughness, and is composed of large particles diameter of spherical shapes. According to previous XRD results, these range on the surface of TiO_2 coating are aggregates of many small TiO_2 crystallites [25].

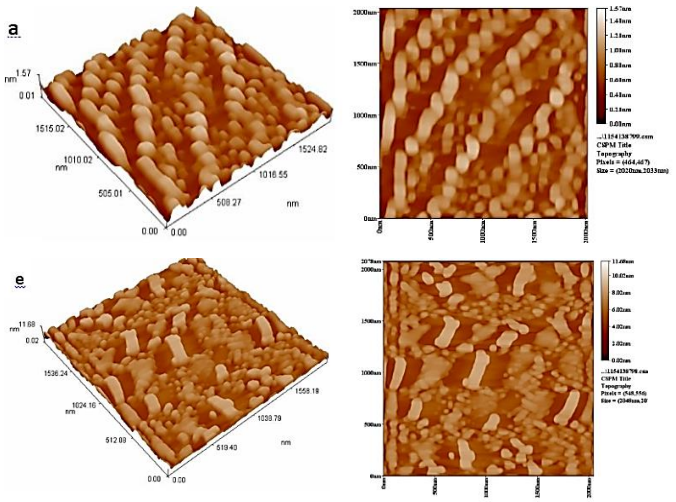

Fig-3 Two- and three-dimensional AFM image of Titanium dioxide (TiO2 nanoparticles calcined at: (a) 500°C, (b) 900°C.

Give images AFM analysis also surface roughness values, as shown in Table 2. means the root of the square roughness (RQ) of the surface of less than (1 nm) and increases with increasing temperature calcinations , which shows the grain of normal forms on the surface. When the temperature increases, the changes in topography and roughness of the paint TIO_2 are largely due to the phase shift of titanium Anatase to rutile and the growth of the crystal TiO_2 [27, 28]. The table shows (1) that the roughness values increase with increasing temperature calcination. After calcined up to 900 ° C, it observed a significant increase in grain size and RQ to 1.22 nm. It is

because the shift from titanium Anatase phase peak toward Rutile phase peak went through a total of smaller particles and the formation of larger particles (J. Yu Yu, is, Jiang, 2002), which then increased its grain size. This result is in agreement with Jimmy C Yu, *et al.* [29] and Jiaguo Yu, *et al.* [30] references.

Table 4. The relationship between roughness values and calcination temperature.

Calcination temperature. (°C)	*Sq. (Root mean square) (nm)*
500	0.206
900	1.22

3.6 Fourier Transform Infrared (FTIR) Analysis

FTIR spectrum shows a wide band range (3400-4000) cm^{-1} which is contribution to the H-O-H stretching mode of the surface adsorbed H_2O molecule and also due to the reaction between the O-H groups of TiO_2 [31]. This OH^- adsorbate plays an important role in photoreceptor stimulation by trapping charge carriers to produce OH reaction radicals, which are the driving force behind the process. Furthermore, they act as adsorbents and activating sites for reacting molecules or contaminants [32]. Another band of around (1620-1640) cm^{-1} is attributed to the H-O-H bending mode. These results agreed with Huang *et al.* [33] and Thangavelu *et. al.* [34]. FTIR results of TiO_2 nanoparticles calcined at (400, 500 and 600) °C showed a broad band at 3419 cm^{-1} and 1634 cm^{-1} due to the stretching and deformation vibrations of surface adsorbed water and hydroxyl groups in the surface of TiO_2. Whereas, TiO_2 calcined at 900 °C did not show any aforesaid two broad peaks and it completely disappeared at high calcination temperature. That led to reduced surface area, pore volume and adsorbed water molecule at high calcinations temperature.

All the samples showed the foremost vibration bands around (500-900) cm^{-1} due to the Ti-O-Ti bond-stretching mode, which indicates the formation of a Titanium oxide [35].

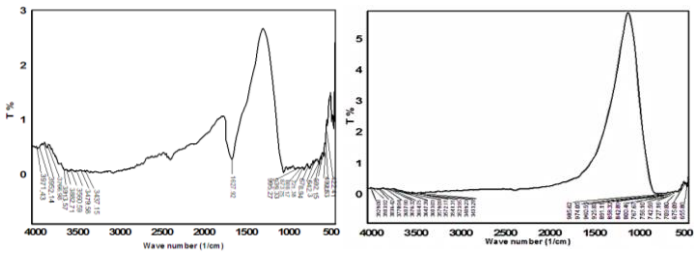

Fig-4 FTIR spectra of the TiO2 nanoparticles calcined at, a) 500˚C, b) 900°C

3.7 Photocatalysis activity

The photocatalytic activity was evaluated by photocatalytic oxidation of Potassium permanganate ($KMnO_4$) under direct sunlight irradiation, by measuring the degradation of Potassium permanganate ($KMnO_4$) under direct sunlight irradiation. UV-Visible Spectrophotometry demonstrated the absorbance value for different film samples with Potassium permanganate after exposure to UV- irradiation from sunlight. Spectrum shown in Figure 5 demonstrates the relationship between the absorbance values and exposure time of irradiation in (hr.). The color of Potassium permanganate dye gradually reduces and finally it completely disappears which means the dye is completely degraded .

The results illustrate calcination temperate effect on the degradation of the dye [36]. It demonstrates that TiO_2 with pure anatase phase exhibit higher photocatalytic activity compared with TiO_2 with pure rutile that needs more time to degrade the dye. This perhaps is due to the higher adsorptive affinity of anatase surface and lower recombination rate of electron–hole pairs as compared to rutile [37]. At high calcination temperatures (900°C), the rutile crystallite size increased due to aggregation under direct sunlight irradiation. The electron generated was permanently trapped in the larger rutile crystallites aggregates, which results in increasing electron–hole recombination rate and decreasing photocatalytic activity. In addition, the growth of TiO_2 crystallites at higher calcination temperature, results in a significant decrease in the surface area. TiO_2 calcined at 800°C shows the highest photocatalytic activity. This is because its' composed of both anatase and rutile phases. The photo-generated electrons transfered from the anatase to the rutile phase may have reduced the rate of electron–hole combination and thus enhanced the photoactivity.

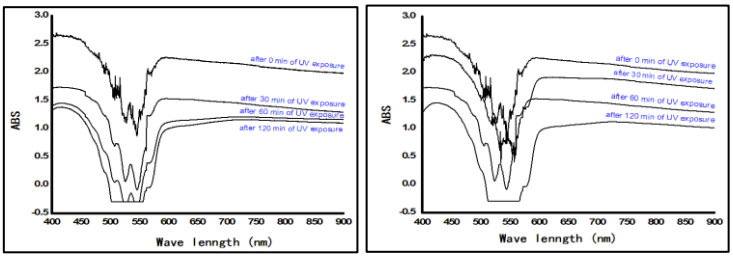

Fig-5: Illustrates the relationship between absorbance and wavelength for TiO2 nanoparticle calcined at a) 500 ˚C, b) 900 °C, measured befor irradation by sunlight (0 min) and after 30, 60, and 120 min exposure to direct sunlight.

4 Conclusions

TiO_2 NP's were synthesis by sol- gel technique at various calcinations temperatures, and then deposited on a glass substrate by spin coating method. The XRD pattern of calcined TiO_2 nanoparticles shows the sharp picks that reveals

the anatase crystalline phase at 500 °C, and rutile phase at 900 °C.

Self-cleaning properties of the prepared nanoparticles were characterized by Water Contact Angle (WCA) and photocatalysis activity. WCA show that the anatase and mixed phase are super-hydrophobic surfaces with WCA of zero value, while rutile phase shows good hydrophilicity with WCA of 7.775.

Acknowledgement

The authors would like to thank the University of Technology, Department of Building and Construction Engineering, and Nanotechnology and Advanced Materials Research Center (Iraq) for help to work on this search.

References

1. Edgerton, S. A., Holdren, M. W., Smith, D. L., & Shah, J. J. (1989). Inter-urban comparison of ambient volatile organic compound concentration in U.S. cities. Journal of the Air Pollution Control Association (JAPCA), 39(5), 729–32.
2. Sweet, C. W., & Vermette, S. J. (1992). Toxic volatile organic compounds in urban air in Illinois. Environmental Science & Technology, 26(1), 165–173. http://doi.org/10.1021/es00025a020
3. Kostiainen, R. (1995). Volatile organic compounds in the indoor air of normal and sick houses. Atmospheric Environment, 29(6), 693–702.
4. Mukund, R., Kelly, T. J., & Spicer, C. W. (1996). Source attribution of ambient air toxic and other VOCs in Columbus, Ohio. Atmospheric Environment, 30(20), 3457–3470. Retrieved from 10.1016/1352-2310(95)00487-4
5. Alberici, R. M., & Jardim, W. F. (1997). Photocatalytic destruction of VOCs in the gas-phase using titanium dioxide. Applied Catalysis B: Environmental, 14(1–2), 55–68. http://doi.org/http://dx.doi.org/10.1016/S0926-3373(97)00012-X.
6. Chun, H., Park, S., You, S., Kang, G., Bae, W., Kim, K., Park, J. E., Öztürk, A., Shin, D. (2009). Preparation of a transparent hydrophilic TiO 2 thin film photocatalyst. Journal of Ceramic Processing Research, 10(2), 219–223.
7. Adawiya J. Haider, Zainab N. Jameel, Samar Y. Taha (2015). Synthesis and Characterization of TiO2 Nanoparticles via Sol-Gel Method by Pulse Laser Ablation. Eng. & Tech. Journal Vol.33 part (B).No.5, p. 761-771.
8. Yu, J. (2003). Preparation and characterization of highly photoactive nanocrystalline TiO2 powders by solvent evaporation-induced crystallization method. Science in China Series B, 46(6), 549. http://doi.org/10.1360/03yb0012
9. Fujishima, A., Rao, T. N., & Tryk, D. a. (2000). Titanium dioxide photocatalysis. Journal of Photochemistry and Photobiology C: Photochemistry Reviews, 1(1), 1–21. http://doi.org/10.1016/S1389-5567(00)00002-2
10. Zainab N. Jameel, Adawiya J. Haider,Samar Y. Taha (2014).Synthesis of TiO2 Nanoparticles by Using Sol-Gel Method and its Applications as Antibacterial Agents. Eng. & Tech. Journal Vol. 32. Part (B).No.3, p.418-426.
11. Verdier, T., Coutand, M., Bertron, A., & Roques, C. (2014). Antibacterial Activity of TiO2 Photocatalyst Alone or in Coatings on E. coli: The Influence of Methodological Aspects. Coatings, 4(3), 670–686. http://doi.org/10.3390/coatings4030670
12. Guo, H., Lee, S. C., Li, W. M., & Cao, J. J. (2003). Source characterization of BTEX in indoor microenvironments in Hong Kong. Atmospheric Environment, 37(1), 73–82. http://doi.org/10.1016/S1352-2310(02)00724-0
13. Finlayson-Pitts, B. J., & Jr., J. N. P. (1997). Tropospheric air pollution: ozone, airborne toxics, polycyclic aromatic hydrocarbons, and particles. Science, 276(5315), 1045–1052.
14. Monod, A., Sive, B. C., Avino, P., Chen, T., Blake, D. R., & Rowland, F. S. (2001). Monoaromatic compounds in ambient air of various cities: a focus on correlations between the xylenes and ethylbenzene. Atmospheric Environment, 35(1), 135–149.
15. Convertino, A., Leo, G., Striccoli, M., Di Marco, G., & Curri, M. L. (2008). Effect of shape and surface chemistry of TiO2 colloidal nanocrystals on the organic vapor absorption capacity of TiO2/PMMA composite.Ba-abbad, M. M., Kadhum, A. A. H., Mohamad, A. B., & Takriff, M. S. (2012). Synthesis and Catalytic Activity of TiO2 Nanoparticles for Photochemical Oxidation of Concentrated Chlorophenols under Direct Solar Radiation. International Journal of ELECTROCHEMICAL SCIENCE, 7, 4871–4888. Retrieved from www.electrochemsci.org
16. Zainab N. Jameel, Adawiya J. Haider, Samar Y. Taha , Shubhra Gangopadhyay and Sangho Bok. (2016) .Evaluation of Hybrid Sol-gel Incorporated with Nanoparticles as Nano Paint., AIP Conf. Proc. 1758, 020001-1–020001-14; http://doi: 10.1063/1.4959377.
17. McCullagh, C., Robertson, J. C., Bahnemann, D., & Robertson, P. J. (2007). The application of TiO2 photocatalysis for disinfection of water contaminated with pathogenic micro-organisms: a review. Research on Chemical Intermediates, 33(3-5), 359–375. http://doi.org/10.1163/156856707779238775
18. Sirimahachai, U., Phongpaichit, S., & Wongnawa, S. (2009). Evaluation of bactericidal activity of TiO 2 photocatalysts: a comparative study of laboratory-made and commercial TiO 2 samples. Songklanakarin J Sci Technol, 31(5), 517–525.
19. Chen, L., Graham, M. E., Li, G., Gentner, D. R., Dimitrijevic, N. M., & Gray, K. A. (2009). Photoreduction of CO2 by TiO2 nanocomposites synthesized through reactive direct current magnetron sputter deposition. Thin Solid Films, 517(19), 5641–5645. http://doi.org/http://dx.doi.org/10.1016/j.tsf.2009.02.075
20. Fujishima, A., Zhang, X., & Tryk, D. A. (2008). TiO 2 photocatalysis and related surface phenomena. Surface Science Reports, 63(12), 515–582.
21. Gao, K., Zhou, S., & Zhao, X. (2011). Preparation and Characterization of Zn-Containing Hydroxyapatite/TiO2 Composite Coatings on Ti Alloys. Materials Science Forum, 685, 367–370. http://doi.org/10.4028/www.scientific.net/MSF.685.367
22. Sung-Suh, H. M., Choi, J. R., Hah, H. J., Koo, S. M., & Bae, Y. C. (2004). Comparison of Ag deposition effects on the photocatalytic activity of nanoparticulate TiO2 under visible and UV light irradiation. Journal of Photochemistry and Photobiology A: Chemistry, 163(1-2), 37–44.
23. Taga, Y. (2009). Titanium oxide based visible light photocatalysts: Materials design and applications. Thin Solid Films, 517(10), 3167–3172. http://doi.org/http://dx.doi.org/10.1016/j.tsf.2008.11.087
24. Zieli, B., Grzechulska, J., Grzmil, B., & Morawski, A. W. (2001). Photocatalytic degradation of Reactive Black 5 A comparison between TiO 2 -Tytanpol A11 and TiO 2 -Degussa P25 photocatalysts, 35, 3–9.
25. Jimmy, Y., Yu, J., & Zhao, J. (2002). Enhanced photocatalytic activity of mesoporous and ordinary TiO2 thin films by sulfuric acid treatment. *Applied Catalysis B: Environmental*, *36*(1), 31–43.
26. Malnieks, K., Mezinskis, G., & Pavlovska, I. (2015). Optical , Photocatalytical and Structural Properties of TiO2 -SiO2 Sol-Gel Coatings on High Content SiO2 Enamel Surface. Materials Science, 21(1), 100–104. Retrieved from http://dx.doi.org/10.5755/j01.ms.21.1.5188
27. Reli, M., Kočí, K., Matějka, V., Kovář, P., & Obalová, L. (2012). Effect of Calcination Temperature and Calcination Time on the Kaolinite/TiO2 Composite for Photocatalytic Reduction of Co2. GeoScience Engineering, 58(4), 10–22. http://doi.org/10.2478/v10205-011-0022-2
28. Zhang, H., & Banfield, J. F. (2000). Understanding Polymorphic Phase Transformation Behavior during Growth of Nanocrystalline Aggregates: Insights from TiO2. The Journal of Physical Chemistry B, 104(15), 3481–3487. http://doi.org/10.1021/jp000499j
29. Yu, J., Yu, J. C., Ho, W., & Jiang, Z. (2002). Effects of calcination temperature on the photocatalytic activity and photo-induced super-hydrophilicity of mesoporous TiO2 thin films. New Journal of Chemistry, 26(5), 607–613. http://doi.org/10.1039/B200964A
30. Yu, J. C., Yu, J., Ho, W., & Zhao, J. (2002). Light-induced super-hydrophilicity and photocatalytic activity of mesoporous TiO2 thin films. Journal of Photochemistry and Photobiology A: Chemistry, 148(1-3), 331–339. http://doi.org/10.1016/S1010-6030(02)00060-6

31. Bessekhouad, Y., Robert, D., & Weber, J. V. (2003). Synthesis of photocatalytic TiO2 nanoparticles: optimization of the preparation conditions. Journal of Photochemistry and Photobiology A: Chemistry, 157(1), 47–53. http://doi.org/http://dx.doi.org/10.1016/S1010-6030(03)00077-7
32. Maira, A. ., Coronado, J. ., Augugliaro, V., Yeung, K. ., Conesa, J. ., & Soria, J. (2001). Fourier Transform Infrared Study of the Performance of Nanostructured TiO2 Particles for the Photocatalytic Oxidation of Gaseous Toluene. Journal of Catalysis, 202(2), 413–420. http://doi.org/10.1006/jcat.2001.3301
33. Huang, C., Bai, H., Huang, Y., Liu, S., Yen, S., & Tseng, Y. (2012). Synthesis of neutral SiO 2/TiO 2 hydrosol and its application as antireflective self-cleaning thin film. International Journal of Photoenergy, 2012. http://doi.org/10.1155/2012/620764
34. Thangavelu, K., Annamalai, R., & Arulnandhi, D. (2013). Preparation and Characterization of Nanosized TiO2 Powder by Sol-Gel Precipitation Route. International Journal of Emerging Technology and Advanced Engineering, 3(1), 636–639.
35. Kusmahetiningsih, N., & Sawitri, D. (2012). Application of TiO2 for Self Cleaning in Water Based Paint with Polyethylene Glycol (PEG) as Dispersant. International Conference on Chemical and Material Engineering, 5–10.
36. Liu, G., Zhang, X., Xu, Y., Niu, X., Zheng, L., & Ding, X. (2005). The preparation of Zn2+-doped TiO2 nanoparticles by sol–gel and solid phase reaction methods respectively and their photocatalytic activities. Chemosphere, 59(9), 1367–1371.
37. Riegel, G., & Bolton, J. R. (1995). Photocatalytic Efficiency Variability in TiO2 Particles. The Journal of Physical Chemistry, 99(12), 4215–4224. http://doi.org/10.1021/j100012a050